Hindawi
Journal of Chemistry
Volume 2019, Article ID 2635219, 10 pages
https://doi.org/10.1155/2019/2635219

Research Article

Kinase Inhibitors of Novel Pyridopyrimidinone Candidates: Synthesis and *In Vitro* Anticancer Properties

Nagy M. Khalifa,[1,2] Mohamed A. Al-Omar,[1,3] Hamad M. Alkahtani,[3] and Ahmed H. Bakheit[3,4]

[1] *Drug Exploration & Development Chair (DEDC), Pharmaceutical Chemistry Department, College of Pharmacy, King Saud University, Riyadh 11451, Saudi Arabia*
[2] *Department of Therapeutical Chemistry, National Research Centre, Dokki, Cairo 12622, Egypt*
[3] *Pharmaceutical Chemistry Department, College of Pharmacy, King Saud University, Riyadh 11451, Saudi Arabia*
[4] *Department of Chemistry, Faculty of Science and Technology, Al-Neelain University, Khartoum, Sudan*

Correspondence should be addressed to Nagy M. Khalifa; nagykhalifa@hotmail.com

Received 11 October 2018; Revised 24 January 2019; Accepted 11 February 2019; Published 20 March 2019

Academic Editor: Maria N. D. S. Cordeiro

A new class of pyridopyrimidinone compounds containing different nitrogenous heterocycles were synthesized starting from the key precursor 2-hydrazinyl-5-phenyl-7-(pyridin-3-yl)pyrido[2,3-*d*]pyrimidin-4(3*H*)-one via condensation with series of aromatic aldehydes and cyclization using different reagents as ethyl acetoacetate, ethyl cyanoacetate, diethyl malonate, and ammonium isothiocyanate. The bioassay results showed compound **6** to be highly effective towards three human cancer cell lines (HepG2, PC-3, and HCT-116) *in vitro* with promising activity values (IC_{50}: 0.5 μM) relative to the standard doxorubicin (IC_{50}: 0.6 μM). Kinase inhibitory evaluation of compound **6** displays hopeful inhibitory action against BRAF V600E, EGFR, and PDGFRβ at100 μM. The molecular docking studies supported the initial kinase assay.

1. Introduction

Cancer is a great public health issue characterized by an uncontrolled increase of cancer cells through cell division and the cells undergo modification by their DNA, leading to death [1–3]. Due to drug resistance and the serious effects of treatment by chemotherapy, the use of available chemotherapeutics is often limited [4]. The combination of chemotherapies with several targets increases selectivity, reduces the resistance, and lowers toxicity towards infected and noninfected cells. Heterocycles have emerged as strong scaffolds for numerous biological considerations [5] and represent a significant part in the designing and detection of novel pharmacologically active entities [6]. The pyridopyrimidine compounds are a group of fused heterocycles that possess various pharmacological applications as antitumor, topoisomerase I inhibitor, adenosine kinase inhibitor, growth regulator, antihepatitis C virus, antiinflammatory, antileishmanial, antiviral, antimicrobial, anticonvulsant, antimycobacterial, CNS depressant, antihypertensive, antiallergic, diuretic, tyrosine kinase inhibitor, and calcium channel antagonist [7–16]. Among them, pyrido[2,3-*d*]pyrimidin-4-ones (**A**–**C**) were found to lower cell proliferation in various cancer cell lines through inhibition of various kinases, e.g., TKs, PI3K, and CDK4/6 (Figure 1) [17–19]. In continuation of our earlier studies that involved synthesis of different other substituted pyridopyrimidine compounds [20–22] and based on the structural features of pyrido[2,3-d]pyrimidine, this study is designed to synthesize various groups containing different substituents in the phenyl ring at position 5 of the parent compound pyrido[2,3-d]pyrimidinone to further improve the SAR-relationship for their cytotoxicity and also for their inhibitory activity against TKs, CDK4/6, and PI3K enzymes.

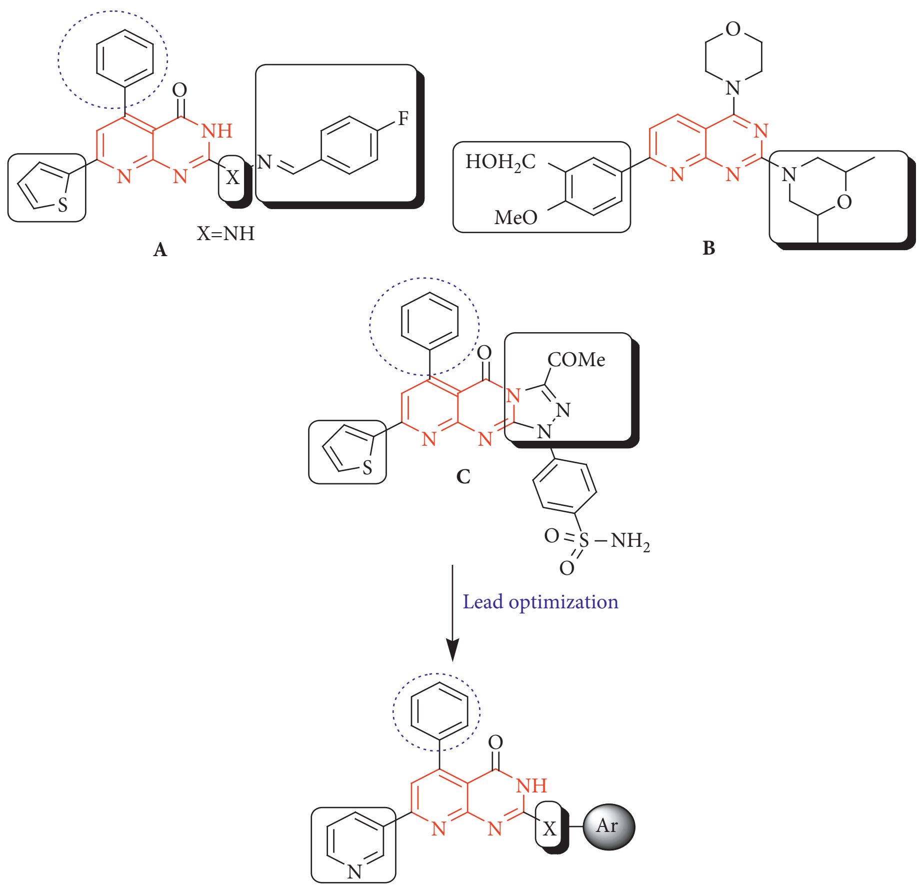

A
B
C

Figure 1: Reported and suggested pyridopyrimidines integrated with kinase inhibitors and anticancer properties.

2. Materials and Methods

2.1. General Information. Electrothermal apparatus with open capillary tubes was used in measuring melting points. Shimadzu 435 IR spectrophotometer was used in measuring IR spectra (KBr). Varian Mercury VX-300 NMR spectrophotometer was used in determining NMR spectra using DMSO-d_6 as a solvent and TMS as internal standard. The proposed structures were within ±0.4% of the theoretical values in microanalyses data. Shimadzu GC/MS-QP 2010 plus spectrometer was used in recording mass spectra.

2.2. Chemistry

2.2.1. 5-Phenyl-7-(pyridin-3-yl)-2-thioxo-2,3-dihydropyrido[2,3-d]pyrimidin-4(1H)-one (**3**). In dry DMF (20 mL), equimolar quantities (0.01 mol) of 6-amino-2,3-dihydro-2-thioxopyrimidin-4(1*H*)-one **1** and α,β-unsaturated ketone **2** were refluxed for 10 h (monitored with TLC). The residue created was gathered and purified from DMF. Yield: 67%; mp: >300°C; IR (KBr, ν_{max}, cm^{-1}): 3327, 3234 (2NH), 1668 (CO), 1178 (CS); ^{1}H NMR (δ, ppm, DMSO-d_6): 7.23–8.65 (m, 10H, Ar), 12.26, 13.01 (2s, 2H, 2NH); ^{13}C NMR (δ, ppm, DMSO-d_6): 108.94, 113.21, 123.87, 127.19, 129.45, 134.59, 135.01, 137.66, 147.82, 149.65, 151.14, 153.02, 153.72, 159.97, 178.01; MS: [*m/z*, 332 (M$^+$)]; Anal. Calcd for: $C_{18}H_{12}N_4OS$ (332.38): C, 65.04; H, 3.64; N, 16.86% Found: C; 64.92, H, 3.57; N, 16.71.

2.2.2. 2-Hydrazinyl-5-phenyl-7-(pyridin-3-yl)pyrido[2,3-d]pyrimidin-4(3H)-one (**4**). In dry ethyl alcohol (30 mL), (0.003 mol) of 2-thioxo derivative **3** and (0.005 mol) of hydrazine hydrate 99% was heated for 12 h. The precipitate created was purified in DMF. Yield: 72%; mp: 286–287°C; IR (KBr, ν_{max}, cm^{-1}): 3446 (NH$_2$), 3362, 3205 (2NH), 1671 (C=O); ^{1}H NMR (δ, ppm, DMSO-d_6): 4.80 (s, 2H, NH$_2$), 7.21–8.73 (m, 10H, Ar), 11.38, 12.76, (2s, 2H, 2NH); ^{13}C NMR (δ, ppm, DMSO-d_6): 118.74, 121.02, 123.90, 126.38, 129.17, 130.01, 134.57, 135.01, 137.21, 147.83, 149.96, 151.93, 152.47, 153.12, 159.97, 162.41; MS: [*m/z*, 330 (M$^+$)]; Anal. Calcd for: $C_{18}H_{14}N_6O$ (330.34): C, 65.44; H, 4.27; N, 25.44% Found: C; 65.29, H, 4.12; N, 25.34.

2.2.3. Synthetic Method for Derivatives (**5a–g**). In glacial acetic acid (10 mL), equimolar amounts of (0.001 mol) of hydrazinyl derivative **4** and several aromatic aldehydes, benzaldehyde, 4-fluorobenzaldehyde, 4-chlorobenzaldehyde, 4-tolylaldehyde, 4-nitrobenzaldehyde, 4-methoxy benzaldehyde, or 4-*N,N*-dimethylamino benzaldehyde were refluxed for 5–8 h. After cooling and pouring into crushed ice, the precipitate obtained was purified in DMF/H$_2$O.

2-[2-Benzylidenehydrazinyl]-5-phenyl-7-(pyridin-3-yl) pyrido[2,3-d]pyrimidin-4(3H)-one (**5a**). Yield: 69%; mp: 336°C; IR (KBr, ν_{max}, cm^{-1}): 3379, 3210 (2NH), 1667 (CO); ^{1}H NMR (δ, ppm, DMSO-d_6): 7.20–8.66 (m, 16H, Ar + =CH), 10.87, 12.68 (2s, 2H, 2NH); ^{13}C NMR (δ, ppm, DMSO-d_6): 116.28, 119.97, 123.64, 127.80, 128.17, 128.63, 129.10, 130.03, 131.14, 132.99, 134.13, 134.49, 139.11, 143.54, 147.68, 149.98, 151.73, 152.71, 153.69, 161.34, 162.15; MS: [*m/z*, 418 (M^+)]; Anal. Calcd for: $C_{25}H_{18}N_6O$ (418.45): C, 71.76; H, 4.34; N, 20.08% Found: C, 71.63; H, 4.17; N, 29.95.

2-[2-(4-Fluorobenzylidene)hydrazinyl]-5-phenyl-7-(pyridin-3-yl)pyrido[2,3-d]pyrimidin-4(3H)-one (**5b**). Yield: 62%; mp: 317°C; IR (KBr, ν_{max}, cm^{-1}): 3365, 3217 (2NH), 1663 (CO); ^{1}H NMR (δ, ppm, DMSO-d_6): 7.15–8.70 (m, 14H, Ar + =CH), 10.78, 12.29 (2s, 2H, 2NH); ^{13}C NMR (δ, ppm, DMSO-d_6): 115.79, 116.25, 119.85, 123.65, 128.13, 128.34, 128.76, 129.16, 130.24, 134.18, 134.59, 140.02, 143.28, 149.55, 150.48, 151.63, 152.69, 153.74, 161.27, 162.18, 164.72; MS: [*m/z*, 436 (M^+)]; Anal. Calcd for: $C_{25}H_{17}FN_6O$ (436.44): C, 68.80; H, 3.93; N, 19.26% Found: C, 68.64; H, 3.79; N, 19.08.

2-[2-(4-Chlorobenzylidene)hydrazinyl]-5-phenyl-7-(pyridin-3-yl)pyrido[2,3-d]pyrimidin-4(3H)-one (**5c**). Yield: 53%; mp: 345°C; IR (KBr, ν_{max}, cm^{-1}): 3381, 3195 (2NH), 1660 (CO); ^{1}H NMR (δ, ppm, DMSO-d_6): 7.23–8.72 (m, 14H, Ar + =-CH), 10.75, 12.36, (2s, 2H, 2NH); ^{13}C NMR (δ, ppm, DMSO-d_6): 116.34, 119.36, 123.60, 128.12, 128.45, 128.84, 129.04, 130.42, 131.56, 134.21, 134.68, 137.13, 140.15, 143.36, 149.47, 150.36, 151.24, 152.72, 153.61, 161.15, 162.19; MS: [*m/z*, 452 (M^+)]; Anal. Calcd for: $C_{25}H_{17}ClN_6O$ (452.9): C, 66.30; H, 3.78; N, 18.56% Found: C, 66.12; H, 3.64; N, 18.39.

2-[2-(4-Methylbenzylidene)hydrazinyl]-5-phenyl-7-(pyridin-3-yl)pyrido[2,3-d]pyrimidin-4(3H)-one (**5d**). Yield: 71%; mp: 321°C; IR (KBr, ν_{max}, cm^{-1}): 3348, 3212 (2NH), 1668 (CO); ^{1}H NMR (δ, ppm, DMSO-d_6): 2.40 (s, 3H, CH_3), 7.20–8.73 (m, 14H, Ar + =CH), 11.05, 12.45, (2s, 2H, 2NH); ^{13}C NMR (δ, ppm, DMSO-d_6): 24.10, 116.87, 119.82, 123.17, 128.05, 128.33, 128.96, 129.15, 130.36, 134.32, 134.59, 140.18, 141.82, 143.62, 149.38, 151.03, 151.46, 152.91, 153.73, 161.22, 162.31; MS: [*m/z*, 432 (M^+)]; Anal. Calcd for: $C_{26}H_{20}N_6O$ (432.48): C, 72.21; H, 4.66; N, 19.43% Found: C, 72.04; H, 4.52; N, 19.28.

2-[2-(4-Nitrobenzylidene)hydrazinyl]-5-phenyl-7-(pyridin-3-yl)pyrido[2,3-d]-pyrimidin-4(3H)-one (**5e**). Yield: 58%; mp: 312°C; IR (KBr, ν_{max}, cm^{-1}): 3365, 3202 (2NH), 1664 (CO); ^{1}H NMR (δ, ppm, DMSO-d_6): 7.21–8.66 (m, 14H, Ar + =CH), 10.82, 12.35 (2s, 2H, 2NH); ^{13}C NMR (δ, ppm, DMSO-d_6): 119.87, 121.17, 123.47, 128.02, 128.66, 129.34, 130.03, 134.45, 134.62, 139.76, 140.16, 143.29, 149.35, 150.29, 151.04, 151.87, 153.04, 153.74, 161.13, 162.25; MS: [*m/z*, 463 (M^+)]; Anal. Calcd for: $C_{25}H_{17}N_7O_3$ (463.45): C, 64.79; H, 3.70; N, 21.16% Found: C, 64.63; H, 3.56; N, 20.98.

2-[2-(4-Methoxybenzylidene)hydrazinyl]-5-phenyl-7-(pyridin-3-yl)pyrido[2,3-d]pyrimidin-4(3H)-one (**5f**). Yield: 73%; mp: 295–296°C; IR (KBr, ν_{max}, cm^{-1}): 3376, 3198 (2NH), 1665 (CO); ^{1}H NMR (δ, ppm, DMSO-d_6): 3.81 (s, 3H, OCH_3), 7.01–8.58 (m, 14H, Ar + =CH), 11.23, 12.56 (2s, 2H, 2NH); ^{13}C NMR (δ, ppm, DMSO-d_6): 56.19, 115.03, 116.89, 119.77, 123.59, 126.09, 128.14, 128.70, 129.15, 130.03, 134.26, 134.71, 140.12, 143.86, 149.27, 151.02, 151.78, 152.42, 153.84, 161.19, 162.34, 165.01; MS: [*m/z*, 448 (M^+)]; Anal. Calcd for: $C_{26}H_{20}N_6O_2$ (448.48): C, 69.63; H, 4.49; N, 18.74% Found: C, 69.47; H, 4.31; N, 18.59.

2-[2-(4-Dimethylaminobenzylidene)hydrazinyl]-5-phenyl-7-(pyridin-3-yl)pyrido[2,3-d]-pyrimidin-4(3H)-one (**5g**). Yield: 75%; mp: 302°C; IR (KBr, ν_{max}, cm^{-1}): 3401, 3234 (2NH), 1660 (CO); ^{1}H NMR (δ, ppm, DMSO-d_6): 2.67 (s, 6H, $2CH_3$), 7.20–8.68 (m, 14H, Ar + =CH), 11.24, 12.58, (2s, 2H, 2NH); ^{13}C NMR (δ, ppm, DMSO-d_6): 42.03, 115.63, 116.85, 119.47, 121.17, 123.57, 128.16, 128.77, 129.16, 130.08, 134.27, 134.45, 140.01, 143.67, 148.99, 151.02, 151.87, 152.04, 152.71, 153.14, 161.17, 162.23; MS: [*m/z*, 461 (M^+)]; Anal. Calcd for: $C_{27}H_{23}N_7O$ (461.52): C, 70.27; H, 5.02; N, 21.24% Found: C, 70.12; H, 4.96; N, 21.08.

2.2.4. Synthetic Method for Derivatives (**6**–**9**). In glacial acetic acid (15 mL), equimolar amounts (0.001 mol) of hydrazinyl derivative **4** and different reagents, namely, ethyl acetoacetate, ethyl cyanoacetate, diethyl malonate, or ammonium isothiocanate were heated for 3–6 h. The mixture was allowed to cool, poured into ice, and the residue obtained was purified in AcOH.

2-(3-Methyl-5-oxo-2,5-dihydro-1H-pyrazol-1-yl)-5-phenyl-7-(pyridin-3-yl)pyrido-[2,3-d]-pyrimidin-4(3H)-one (**6**). Yield: 45%; mp: 302°C; IR (KBr, ν_{max}, cm^{-1}): 3368, 3214 (2NH), 1725, 1660 (2CO); ^{1}H NMR (δ, ppm, DMSO-d_6): 1.87 (s, 3H, CH_3), 7.21–8.65 (m, 11H, Ar + CH-pyrazolone), 10.47, 12.80 (2s, 2H, 2NH); ^{13}C NMR (δ, ppm, DMSO-d_6): 21.57, 106.48, 116.99, 119.91, 123.69, 128.11, 128.48, 129.10, 134.20, 134.58, 140.03, 149.13, 151.01, 151.96, 152.67, 152.84, 153.22, 161.38, 162.45, 172.46; MS: [*m/z*, 396 (M^+)]; Anal. Calcd for: $C_{22}H_{16}N_6O_2$ (396.4): C, 66.66; H, 4.07; N, 21.20% Found: C, 66.52; H, 3.94; N, 21.06.

2-(3-Amino-5-oxo-2,5-dihydro-1H-pyrazol-1-yl)-5-phenyl-7-(pyridin-3-yl)pyrido-[2,3-d]-pyrimidin-4(3H)-one (**7**). Yield: 60%; mp: 310°C; IR (KBr, ν_{max}, cm^{-1}): 3431 (NH_2), 3346, 3196 (2NH), 1730, 1667 (2CO); ^{1}H NMR (δ, ppm, DMSO-d_6): 4.58 (s, 2H, NH_2), 7.24–8.78 (m, 11H, Ar + CH-pyrazolone), 11.53, 12.39 (2s, 2H, 2NH); ^{13}C NMR (δ, ppm, DMSO-d_6): 106.75, 116.85, 119.65, 123.16, 128.05, 128.36, 129.18, 134.42, 134.81, 140.08, 149.01, 150.37, 151.90, 152.65, 153.12, 161.09, 163.14, 171.82; MS: [*m/z*, 397 (M^+)]; Anal. Calcd for: $C_{21}H_{15}N_7O_2$ (397.39): C, 63.47; H, 3.80; N, 24.67% Found: C, 63.31; H, 3.65; N, 24.58.

1-[4-Oxo-5-phenyl-7-(pyridin-3-yl)-3,4-dihydropyrido [2,3-d]pyrimidin-2-yl]pyrazolidine-3,5-dione (**8**). Yield: 39%; mp: 349°C; IR (KBr, ν_{max}, cm^{-1}): 3420, 3210 (2NH), 1705, 1682, 1667 (3CO); ^{1}H NMR (δ, ppm, DMSO-d_6): 2.98 (s, 2H, CH_2), 7.22–8.71 (m, 10H, Ar), 11.84, 12.59 (2s, 2H, 2-NH); ^{13}C NMR (δ, ppm, DMSO-d_6): 90.21, 116.93, 119.73, 123.34, 127.91, 128.41, 129.30, 134.59, 134.66, 140.03, 149.28, 151.13, 151.86, 152.74, 153.21, 161.02, 163.18, 167.49, 170.56; MS: [*m/z*, 398 (M^+)]; Anal. Calcd for: $C_{21}H_{14}N_6O_3$ (398.37): C, 63.31; H, 3.54; N, 21.10% Found: C, 63.17; H, 3.39; N, 20.91.

3-Amino-6-phenyl-8-(pyridin-3-yl)pyrido[2,3-d]triazolo [4,3-a]pyrimidin-5(1H)-one (**9**). Yield: 63%; mp: 347°C; IR (KBr, ν_{max}, cm^{-1}): 3460 (NH_2), 3317 (NH), 1669 (CO); ^{1}H NMR (δ, ppm, DMSO-d_6): 5.60 (s, 2H, NH_2), 7.23–8.76 (m,

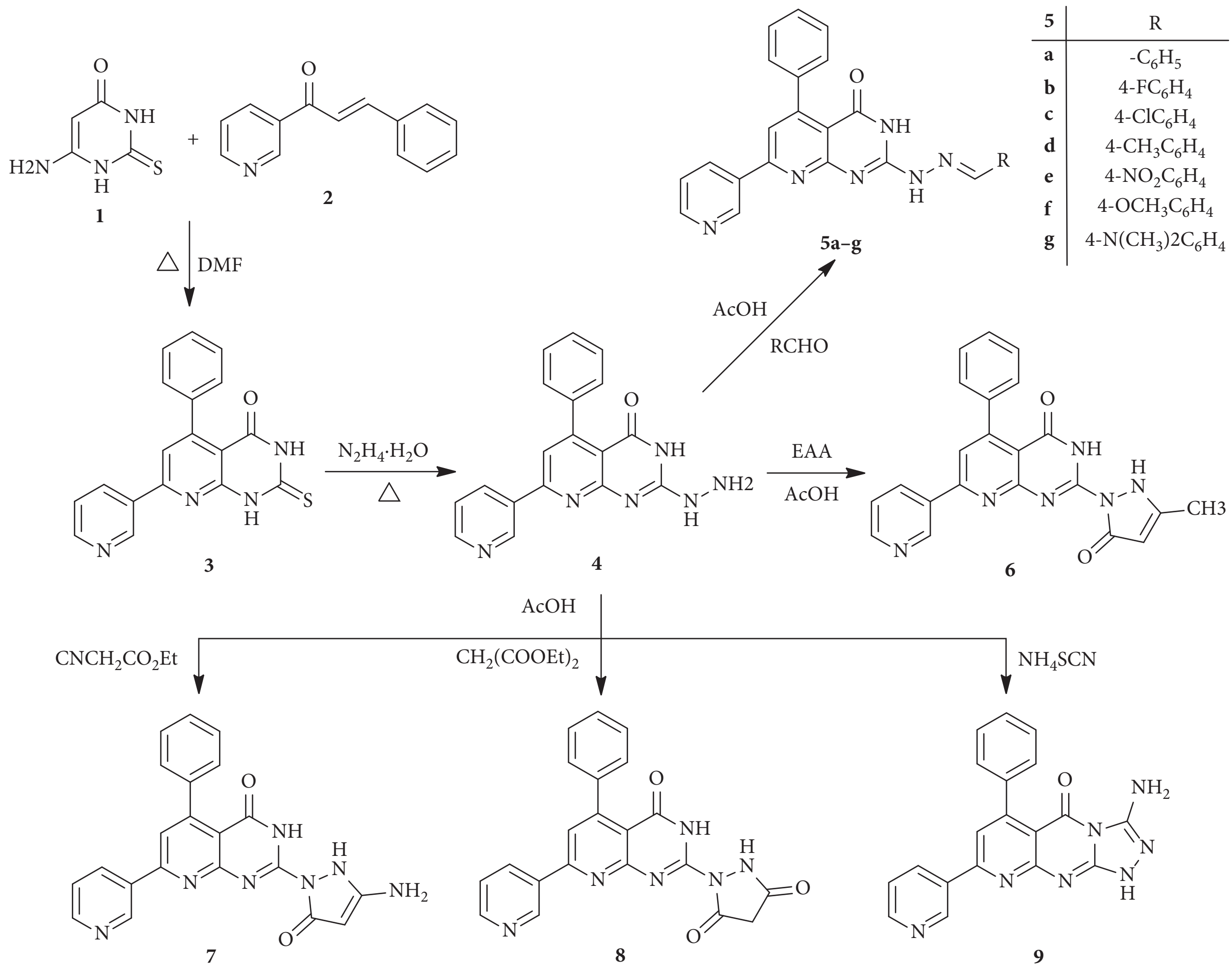

Scheme 1: Synthetic pathway for pyridopyrimidines (**3**–**9**).

10H, Ar), 12.55 (s, 1H, NH); ^{13}C NMR (δ, ppm, DMSO-d_6): 117.30, 119.58, 123.79, 127.98, 129.01, 129.57, 134.25, 134.76, 139.53, 148.95, 151.06, 151.90, 152.64, 153.42, 155.47, 160.37, 161.77; MS: [m/z, 355 (M^+)]; Anal. Calcd for: $C_{19}H_{13}N_7O$ (355.35): C, 64.22; H, 3.69; N, 27.59% Found: C, 64.06; H, 3.54; N, 27.43.

3. Results and Discussion

3.1. Chemistry. A group of substituted pyridopyrimidines were obtained via treatment of starting **1** with α,β-unsaturated ketone **2** in dry DMF to afford 2-thioxo derivative **3**. IR spectrum of **3** revealed four strong bands at 3327, 3234, 1668, and 1178 cm^{-1} due to 2NH, CO, and CS functions, respectively. In the same time, ^{1}HNMR spectrum displayed two singlets at δ 12.26 and 13.01 ppm assignable for 2NH protons. Also, ^{13}CNMR spectrum showed signal at 178.01 ppm for C=S carbon. Treatment of hydrazine hydrate with thioxo derivative **3** afforded the corresponding 2-hydrazinyl derivative **4**. IR spectrum of **4** revealed four peaks at 3446, 3362, 3205, and 1671 cm^{-1} attributed to amino, two amides, and carbonyl functions, respectively. Moreover, ^{1}H NMR spectrum confirmed the presence of amino and amide protons by existence of three singlet peaks at δ 4.80, 11.38, and 12.76 ppm. The MS revealed [M^+] at m/z 330 agreed with the MF $C_{18}H_{14}N_6O$. Compound **4** was allowed to react with different aromatic aldehydes to afford 2-arylidene derivatives **5a**–**g**. Compounds **5a**–**g** were confirmed on the basis of their IR spectra and showed strong peaks around the regions 3401–3348, 3234–3195, and 1668–1660 cm^{-1} corresponding to two amide and carbonyl functions. Furthermore, the methine functions were proved by presence of singlet peaks in the aromatic region in ^{1}H NMR spectrum and signals around 143 ppm in ^{13}H NMR spectrum.

Treatment of the 2-hydrazinyl intermediate **4** with active methylene, namely, ethyl acetoacetate, ethyl cyanoacetate, diethyl malonate, or ammonium isothiocyanate afforded the corresponding 5-substituted pyrazolones and triazolopyrimidines **6**–**9** (Scheme 1). The new pyrazolone ring linked to the pyridopyrimidine backbone in compound **6** was proved with the appearance of strong bands at 3214 and 1725 cm^{-1} referred to NH and CO functions of the pyrazole ring in IR spectrum and existence of two singlet peaks at δ 1.87 and 10.87 ppm due to methyl attached to the pyrazole ring and -NH protons. The molecular formula $C_{18}H_{14}N_6O$ of **6** was confirmed by the presence of molecular ion peak [M^+] at m/z 330 in MS.

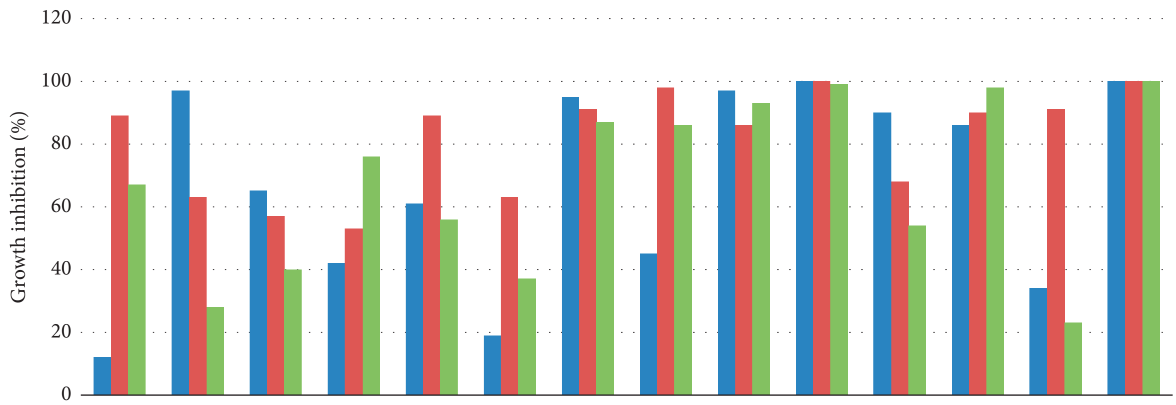

	3	4	5a	5b	5c	5d	5e	5f	5g	6	7	8	9	Doxorubicin
HepG2	12	97	65	42	61	19	95	45	97	100	90	86	34	100
PC-3	89	63	57	53	89	63	91	98	86	100	68	90	91	100
HCT-116	67	28	40	76	56	37	87	86	93	99	54	98	23	100

Compound number

Figure 2: Percentage of growth inhibition activity against cancer cell lines at 100 μM dose.

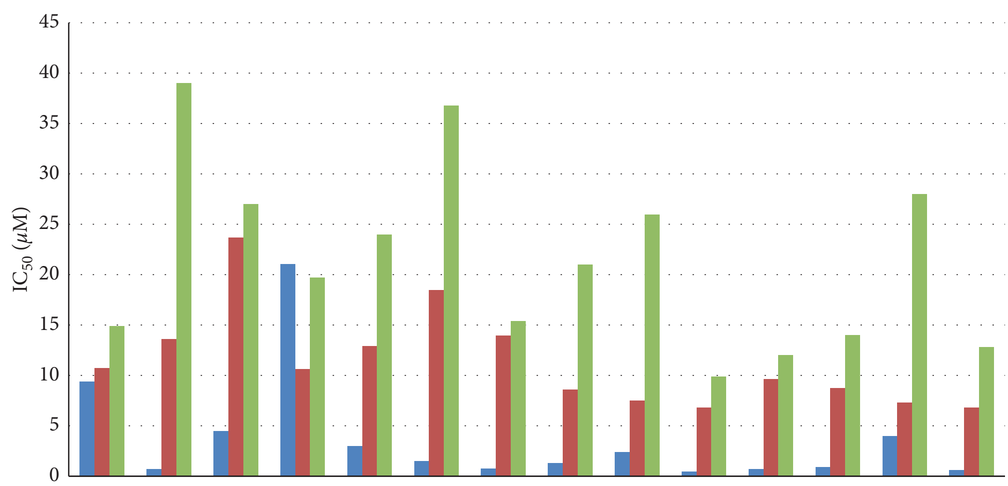

	3	4	5a	5b	5c	5d	5e	5f	5g	6	7	8	9	Doxorubicin
HepG2	9.4	0.7	4.5	21.07	3	1.5	0.8	1.3	2.4	0.5	0.7	0.9	4.01	0.6
PC-3	10.76	13.61	23.7	10.65	12.9	18.5	13.98	8.6	7.5	6.82	9.65	8.76	7.3	6.8
HCT-116	14.9	39	27	19.7	24	36.8	15.4	21	26	9.9	12	14	28	12.8

Compound number

Figure 3: IC_{50} of the tested compounds against cancer cell lines.

IR spectrum of compound **7** confirmed attachment of the new 3-aminopyrazolone ring to the original backbone by the presence of broad bands at 3431, 3196, and 1730 cm^{-1} due to $-NH_2$, -NH, and CO functions of the new moiety, respectively, besides other bands at 3346 and 1667 cm^{-1} for NH and CO functions of pyridopyrimidine. Also, ^{1}H NMR spectrum proved the presence of the new aminopyrazolone ring by the existence of two singlet peaks at δ 4.58 and 11.53 ppm corresponding to amino and amide protons. The appearance of molecular ion peak $[M^+]$ at *m/z* 397 proved the molecular formula $C_{21}H_{15}N_7O_2$ of **7** in MS.

On the contrary, the new pyrazolidine-3,5-dione ring in compound **8** was proved by the existence of strong bands at 3210, 1705, and 1682 cm^{-1} referred to NH and 2 CO functions in the IR spectrum. The methylene group of the new ring appeared as a singlet peak at δ 2.98 ppm in ^{1}H NMR spectrum and signal at 90.21 ppm in ^{13}H NMR spectrum. MS gave a $[M^+]$-ion peak at *m/z* 398 equivalents to the molecular formula $C_{21}H_{14}N6_6O_3$.

Table 1: Percentage of kinase inhibition of derivative **6** at 100 μM.

Kinase	Compound 6 % Inhibition
AKT1	−79
AKT2	−85
BRAF (V600E)	−91
CDK2/cyclin A1	−78
CHK1	−6
EGFR	−97
PDGFRβ	−94
c-RAF	37

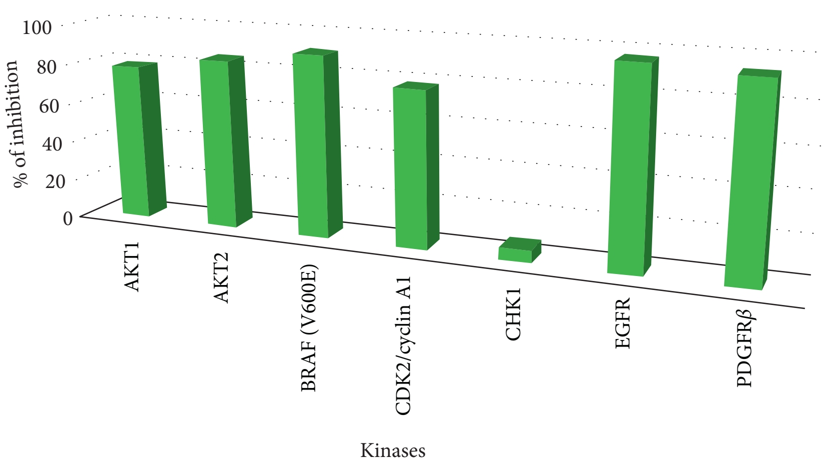

Figure 4: % of kinase inhibition of target molecule **6**.

Finally, the new 3-aminotriazole ring fused with pyridopyrimidine moiety in **9** was proved in the IR spectra by the existence of bands at 3460 and 3317 cm^{-1} referred to NH_2 and NH functions besides other band at 1669 cm^{-1} due to carbonyl of pyridopyrimidine moiety. ^{1}H NMR spectrum displayed two singlets at 5.60 and 12.55 attributed to NH_2 and NH protons of the new fused ring. ^{13}C NMR spectrum displayed the carbons at their expected regions, and MS gave a [M$^+$]-ion peak at *m/z* 355 equivalents to the molecular formula of **9**.

3.2. Biology

3.2.1. In Vitro Cytotoxic Screening against HepG2, PC-3, and HCT-116 Cell Lines. Anticancer evaluation of the newly obtained products represented in Figure 2 was screened against three human cancer cell lines (HepG2, PC3, or HCT-116) [23]. The tested compounds that displayed inhibitory effect more than 90% referring doxorubicin as a standard drug (IC_{50} 0.6 μM) were chosen for IC_{50} examination (concentrations required for 50% inhibition of cell viability). The *in vitro* screening of compounds **3**–**9** at 100 μM (Figure 3) exhibited remarkable anticancer activities, and compound **6** showed promising potency against hepatic cancer cell line (anti-HepG2) with ($IC_{50} = 0.5\,\mu$M).

3.2.2. Structure-Activity Relationships. The cytotoxic screening results revealed that thioxo precursor **3** displayed poor anticancer activity against all cancer cell lines. Upon converting the thioxo group in **3** to hydrazide in **4**, antihepatic cancer (HepG2) effect was greatly increased as a result of the presence of the hydrophilic electron-rich nature in compound **4** which causes the electron factor to give a positive impact on the antiproliferative properties. Attachment of the pyrazole ring as a substituent at position 2 of the backbone moiety as in compounds **6**, **7,** and **8** afforded the highest potency of anticancer activity. Compound **6** that carried 5-methyl-3-oxopyrazole exhibited the highest activity against all the tested cell lines. The activity was reduced and shifted toward the PC-3 cell line after replacement of the 5-methyl-3-oxo-pyrazole nucleus at 6 by 3-amino-5-oxopyrazol in 7. Upon replacing the mentioned pyrazole moiety in **6** by 3,5-dioxopyrazole in **8**, or by fused triazolo[4,3-a]pyrimidine in **9**, the activity profile was changed.

3.2.3. Kinase Inhibition Screening. According to the data of cytotoxic assay, the highly potent derivative **6** was chosen for *in vitro* inhibition assessment against a list of different protein, AKT1, AKT2, BRAF (V600E), CDK2/cyclin A1, CHK1, EGFR, PDGFRβ, and c-RAF kinases at 100 μM utilized the radiometric or ADP-Glo assay procedure. Three of the tested kinases (BRAF V600E, EGFR, and PDGFRβ)

Table 2: Molecular simulation results for ACV/PNV interactions with HAS.

Ligand	Receptor	Amino acid residues	Interaction type	Distance (Å)	Total binding energy (kcal·mol^{-1})	RMSD
Compd. **6**	EGFR (4HJO)	LEU 694	pi-H	3.47	−6.156	1.878
		MET 769	H-acceptor	3.86		
	CDK6 (5L2I)	VAL 101	H-acceptor	3.52	−6.942	1.251
		LYS 147	H-acceptor	3.09		
		VAL 27	pi-H	4.35		

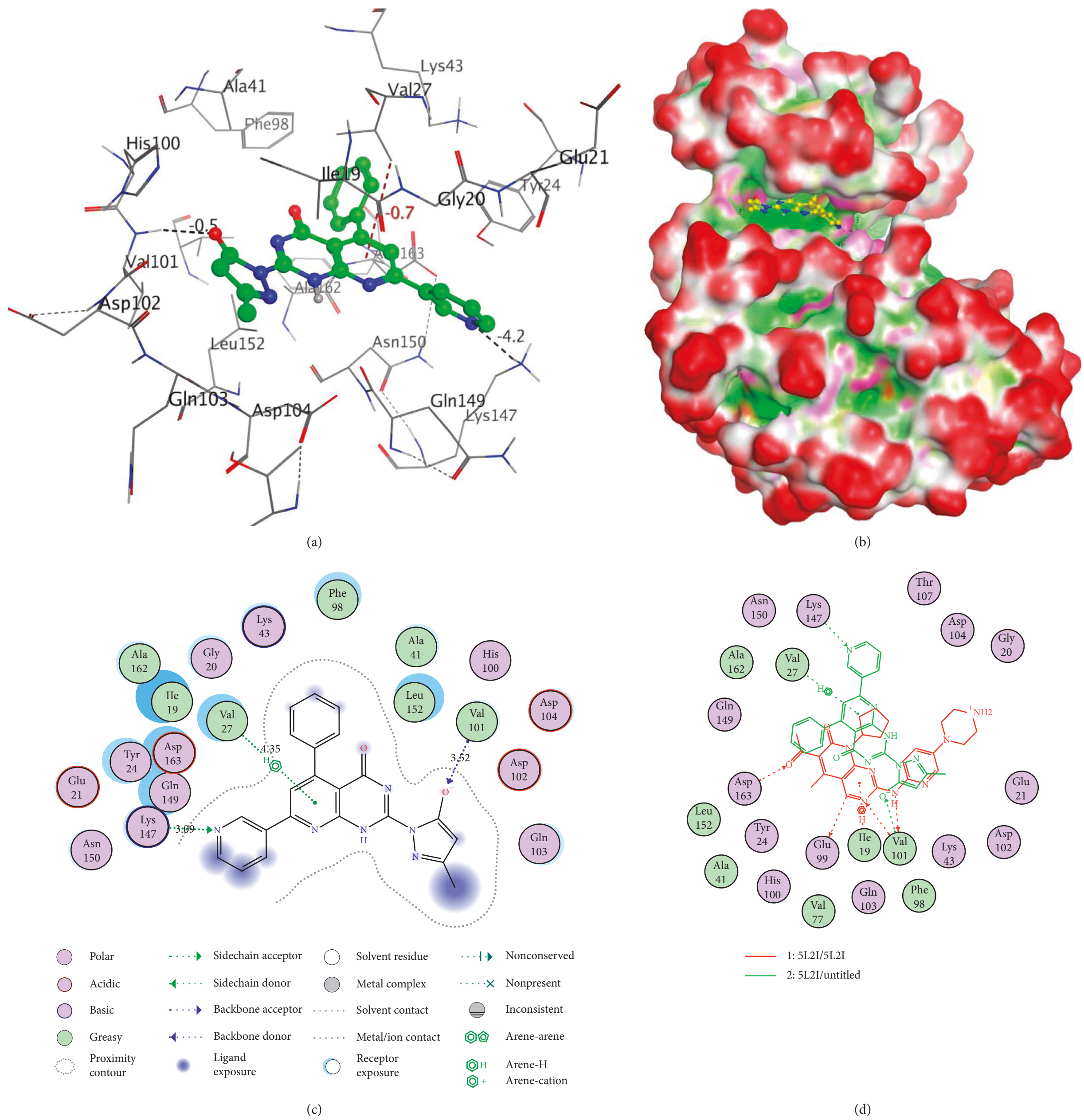

Figure 5: The interaction between compound **6** and CDK6 kinase protein (PDB code: 5L2I), presented by MOE 2015: (a, b) 3D compound **6** binding geometry (yellow sticks) in the CDK6 binding site cavity. (c) 2D interaction diagram of compound **6** with the CDK6 binding site cavity. (d) 2D diagrams of compound **6** (green) and padlbocyclib (red) were overlapping.

were highly inhibited by more than 90% with the highest inhibition recorded with EGFR at 97%. On the contrary, compound **6** appeared to partially activate the c-RAF kinase with a rise in counts of 37% over the control substrate rates (Table 1, Figure 4).

3.2.4. Molecular Docking Study. Molecular docking was used to analyze the supposed binding mode of the designed compound with CDK6 and EGFR to better understand the mechanism of inhibition. For the docking studies, the crystal structure of the complex CDK6 and EGFR has been chosen

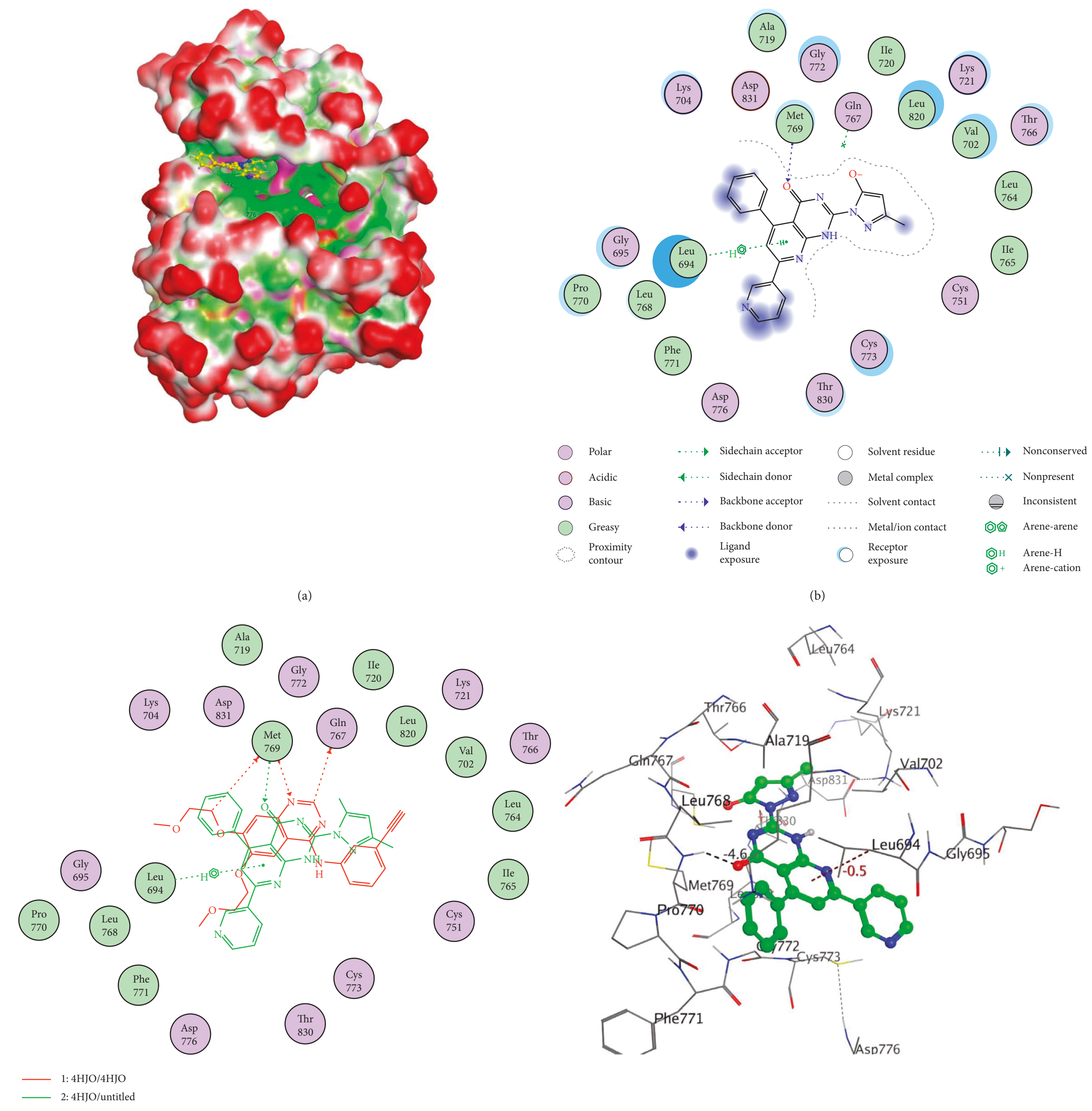

FIGURE 6: The interaction between compound **6** and EGFR kinase protein (PDB code: 4HJO), presented by MOE 2015: (a, d) 3D compound **6** binding geometry (yellow sticks) in the CDK6 binding site cavity. (b) 2D interaction diagram of compound **6** with the CDK6 binding site cavity. (c) 2D diagrams of compound **6** (green) and erlotinib (red) were overlapping.

(PDB code 5L2I [24] and PDB code 4HJO [25]). The most active compound **6** in the current study was docked into the CDK6 and EGFR kinase's putative active site. For the receptor preparation, the Molecular Operating Environment software package MOE® 2015 [26] has been used by means of the removal of water molecules and the addition of hydrogen atoms. MOE has also been used for the graphic structure of ligands 3D and then saved on data lists after minimizing structure and geometries energy. For each receptor, the pockets were then used to dock ligands after setting London dG to scoring function and GBVI/WSA dG to re scoring function. Therefore, the scoring and RMSD (root-mean-square deviation) values for the best conformation of each ligand with different receptors are shown in Table 2, as well as 2D and 3D figures of each selected conformation are shown in Figures 3 and 4. Docking simulation of compound **6** into kinase domain of CDK6 and EGFR postulated the pivotal function of both the backbone moiety and the side chain substituent (Figures 5 and 6).

4. Conclusions

A library of substituted pyridopyrimidines **3–9** were designed and screened for their cytotoxicity. There are potent growth inhibitory effects against hepatic, prostate, and colon cancer cells lines, in comparison with doxorubicin as positive control. Regarding HepG2 cell line, compound **6** showed the greatest inhibitory activities against hepatic cancer (HepG2) with inhibition percent ($IC_{50} = 0.5\,\mu M$) more potent than doxorubicin ($IC_{50} = 0.6\,\mu M$). A molecular docking study of compound **6** into the ATP binding site of EGFR exhibited identical binding as erlotinib.

Data Availability

The data used to support the findings of this study are available from the corresponding author upon request.

Conflicts of Interest

The authors declare that they have no conflicts of interest.

Acknowledgments

The authors would like to extend their sincere appreciation to the Deanship of Scientific Research at King Saud University for funding this research through Research Group No. RG-320.

Supplementary Materials

The NMR spectrum and elementary analysis data used to support the results of this study are included in the supplementary materials. (*Supplementary Materials*)

References

[1] H.-C. Wu, D. K. Chang, and C.-T. Huang, "Targeted therapy for cancer," *Journal of Molecular Cancer*, vol. 2, pp. 57–66, 2006.

[2] H. Varmus, "The new era in cancer research," *Science*, vol. 312, no. 5777, pp. 1162–1165, 2006.

[3] N. Goodarzi, R. Varshochian, G. Kamalinia, F. Atyabi, and R. Dinarvand, "A review of polysaccharide cytotoxic drug conjugates for cancer therapy," *Carbohydrate Polymers*, vol. 92, no. 2, pp. 1280–1293, 2013.

[4] L.-W. Zheng, Y. Li, D. Ge et al., "Synthesis of novel oxime-containing pyrazole derivatives and discovery of regulators for apoptosis and autophagy in A549 lung cancer cells," *Bioorganic & Medicinal Chemistry Letters*, vol. 20, no. 16, pp. 4766–4770, 2010.

[5] G. Eren, S. Ünlü, M.-T. Nuñez et al., "Synthesis, biological evaluation, and docking studies of novel heterocyclic diaryl compounds as selective COX-2 inhibitors," *Bioorganic & Medicinal Chemistry*, vol. 18, no. 17, pp. 6367–6376, 2010.

[6] M. E. Welsch, S. A. Snyder, and B. R. Stockwell, "Privileged scaffolds for library design and drug discovery," *Current Opinion in Chemical Biology*, vol. 14, no. 3, pp. 347–361, 2010.

[7] K. Horváti, B. Bacsa, N. Szabó et al., "Antimycobacterial activity of peptide conjugate of pyridopyrimidine derivative against *Mycobacterium tuberculosis* in a series of in vitro and in vivo models," *Tuberculosis*, vol. 95, pp. S207–S211, 2015.

[8] J.-P. Zhang, J. Huang, C. Liu et al., "Discovery of a series of pyridopyrimidine derivatives as potential topoisomerase I inhibitors," *Chinese Chemical Letters*, vol. 25, no. 7, pp. 1025–1028, 2014.

[9] A. C. Krueger, D. L. Madigan, D. W. Beno et al., "Novel hepatitis C virus replicon inhibitors: synthesis and structure activity relationships of fused pyrimidine derivatives," *Bioorganic & Medicinal Chemistry Letters*, vol. 22, no. 6, pp. 2212–2215, 2012.

[10] T. Saurat, F. Buron, N. Rodrigues et al., "Design, synthesis, and biological activity of pyridopyrimidine scaffolds as novel PI3K/mTOR dual inhibitors," *Journal of Medicinal Chemistry*, vol. 57, no. 3, pp. 613–631, 2014.

[11] K. Malagu, H. Duggan, K. Menear et al., "The discovery and optimisation of pyrido[2,3-d]pyrimidine-2,4-diamines as potent and selective inhibitors of mTOR kinase," *Bioorganic & Medicinal Chemistry Letters*, vol. 19, no. 20, pp. 5950–5953, 2009.

[12] M. A. Matulenko, C.-H. Lee, M. Jiang et al., "5-(3-Bromophenyl)-7-(6-morpholin-4-ylpyridin-3-yl)pyrido[2,3-d]pyrimidin-4-ylamine: structure-activity relationships of 7-substituted heteroaryl analogs as non-nucleoside adenosine kinase inhibitors," *Bioorganic & Medicinal Chemistry*, vol. 13, no. 11, pp. 3705–3720, 2005.

[13] B. Veeraswamy, D. Madhu, G. Jitender Dev et al., "Studies on synthesis of novel pyrido[2,3-*d*]pyrimidine derivatives, evaluation of their antimicrobial activity and molecular docking," *Bioorganic & Medicinal Chemistry Letters*, vol. 28, no. 9, pp. 1670–1675, 2018.

[14] R. Naresh Kumar, G. Jitender Dev, N. Ravikumar et al., "Synthesis of novel triazole/isoxazole functionalized 7-(trifluoromethyl)pyrido[2,3-*d*]pyrimidine derivatives as promising anticancer and antibacterial agents," *Bioorganic & Medicinal Chemistry Letters*, vol. 26, no. 12, pp. 2927–2930, 2016.

[15] J. Hou, S. Wan, G. Wang et al., "Design, synthesis, anti-tumor activity, and molecular modeling of quinazoline and pyrido [2,3-*d*]pyrimidine derivatives targeting epidermal growth factor receptor," *European Journal of Medicinal Chemistry*, vol. 118, pp. 276–289, 2016.

[16] C. Kurumurthy, P. Sambasiva Rao, B. Veera swamy et al., "Synthesis of novel alkyltriazole tagged pyrido[2,3-*d*]pyrimidine derivatives and their anticancer activity," *European Journal of Medicinal Chemistry*, vol. 46, no. 8, pp. 3462–3468, 2011.

[17] L. Cordeu, E. Cubedo, E. Bandrés et al., "Biological profile of new apoptotic agents based on 2,4-pyrido[2,3-*d*]pyrimidine derivatives," *Bioorganic & Medicinal Chemistry*, vol. 15, no. 4, pp. 1659–1669, 2007.

[18] C. Sanmartín, M. V. Domínguez, L. Cordeu et al., "Synthesis and biological evaluation of 2,4,6-functionalized derivatives of pyrido[2,3-*d*]pyrimidines as cytotoxic agents and apoptosis inducers," *Archiv der Pharmazie*, vol. 341, no. 1, pp. 28–41, 2008.

[19] M. Font, Á. González, J. A. Palop, and C. Sanmartín, "New insights into the structural requirements for pro-apoptotic agents based on 2,4-diaminoquinazoline, 2,4-diaminopyrido [2,3-d]pyrimidine and 2,4-diaminopyrimidine derivatives," *European Journal of Medicinal Chemistry*, vol. 46, no. 9, pp. 3887–3899, 2011.

[20] H. S. A. Elzahabi, E. S. Nossier, N. M. Khalifa, R. A. Alasfoury, and M. A. El-Manawaty, "Anticancer evaluation and molecular modeling of multi-targeted kinase inhibitors based pyrido[2,3-*d*]pyrimidine scaffold," *Journal of Enzyme*

Inhibition and Medicinal Chemistry, vol. 33, no. 1, pp. 546–557, 2018.

[21] N. M. Khalifa, E. S. Nossier, and A. E. Amr, "Efficient synthesis and reactions of new functionally substituted pyrido [2,3-d]pyrimidine candidates," *Russian Journal of General Chemistry*, vol. 88, no. 6, pp. 1228–1231, 2018.

[22] N. M. Khalifa, M. A. Al-Omar, H. M. Alkahtani, and A. H. Bakheit, "Pyrido[2,3-d]pyrimidine as anticancer agents," US Patent 10,100,054 B1, 2018.

[23] T. Mosmann, "Rapid colorimetric assay for cellular growth and survival: application to proliferation and cytotoxicity assays," *Journal of Immunological Methods*, vol. 65, no. 1-2, pp. 55–63, 1983.

[24] P. Chen, N. V. Lee, W. Hu et al., "Spectrum and degree of CDK drug interactions predicts clinical performance," *Molecular Cancer Therapeutics*, vol. 15, no. 10, pp. 2273–2281, 2016.

[25] J. H. Park, Y. Liu, M. A. Lemmon, and R. Radhakrishnan, "Erlotinib binds both inactive and active conformations of the EGFR tyrosine kinase domain," *Biochemical Journal*, vol. 448, no. 3, pp. 417–423, 2012.

[26] CCG, *Molecular Operating Environment (MOE)*, Chemical Computing Group Inc., Montreal, QC, Canada, 2015.